Robotica: (2020) volume 38, pp. 118–135. © Cambridge University Press 2019
doi:10.1017/S026357471900050X

Robust Active Disturbance Rejection Control For Flexible Link Manipulator

Raouf Fareh†*, Mohammad Al-Shabi†, Maamar Bettayeb†, ‡ and Jawhar Ghommam¶

† *Department of Mechanical and Nucluar Engineering, College of Engineering, University of Sharjah, UAE*
E-mail: malshabi@sharjah.ac.ae
‡ *MCEIES, King Abdulaziz University, Jeddah, KSA*
E-mail: maamar@sharjah.ac.ae
¶ *Department of Electrical and Computer Engineering, Sultan Qaboos University, Oman*
E-mail: jghommam@gmail.com

(Accepted March 16, 2019. First published online: April 12, 2019)

SUMMARY
This paper presents an advanced robust active disturbance rejection control (ADRC) for flexible link manipulator (FLM) to track desired trajectories in the joint space and minimize the link's vibrations. It has been shown that the ADRC technique has a very good disturbance rejection capability. Both the internal dynamics and the external disturbances can be estimated and compensated in real time. The proposed robust ADRC control law is developed to solve the problems existing in the original version of the ADRC related to the disturbance estimation errors and the variation of the parameters. Indeed, these parameters cannot be included in the existing disturbances and then be estimated by the extended state observer. The proposed control law is based on the sliding mode technique, which considers the uncertainties in the control gains and disturbance estimation errors. Lyapunov theory is used to prove the closed-loop stability of the system. The proposed control strategy is simulated and tested experimentally on one FLM. The effect of the observer bandwidth on the system performance is simulated and studied to select the best values of the bandwidth frequency. The simulation and experimental results show that the proposed robust ADRC has better performance than the traditional ADRC.

KEYWORDS: Flexible link manipulator; Extended state observer (ESO); Sliding mode; Active disturbance rejection control (ADRC); Stability.

1. Introduction

Modeling and control of flexible link manipulators (FLMs) have attracted much attention due to the potential advantages of the flexibility in the arms. The structural flexibility has many advantages over heavy and rigid structure such as lower energy consumption, small actuators to move the link and higher payload to robot weight ratio. The control of the FLMs has many challenges because of the link's flexibility, such as non-minimal phase nature and under-actuation. The non-minimum phase nature occurs due to the non-collocation of actuators and sensors while the under-actuation occurs because of finite number of actuators and infinite degrees of freedom to be controlled. Many classical theories are considered to control a FLM such as optimal control,[1] robust control,[2] feedback linearization,[3] inverse dynamics[4] and singular perturbation theory,[5,6] distributed and hierarchical control.[7,8] Most of the previous and existing control strategies are based on a mathematical description of the robot. However, many real systems are highly uncertain and the accurate mathematical

* Corresponding author. E-mail: rfareh@sharjah.ac.ae

model is usually not available. This creates a dilemma for control design about the possibility to handle these disturbances. Most of the existing methods proposed the disturbance attenuation techniques to solve this problem. Less-known solutions are proposed to estimate and cancel the disturbance directly. Many disturbance estimators have been presented in the literature such as disturbance observer,[9] unknown input observer,[10] perturbation observer[11] and extended state observer (ESO).[12,13] Based on the ESO, a new algorithm called "Active Disturbance Rejection Control" (ADRC) has been developed.[12] The main idea of this control strategy is to actively estimate and compensate the unknown dynamics and the disturbances. In addition, it requires very little information about the plant. Then the controller uses the information needed from the ESO to control the system instead of being dependent on the mathematical model. For FLM, the strategy consists in developing a chain of two integrators supported by a new control variable and a total disturbance from the conventional model of the manipulator. The total disturbance contains the coupling terms, depending on the flexible and rigid parts of the FLM. Then the proposed control law compensates the existing disturbance to perfectly track the desired trajectories. Consequently, the control input can be considered as a combination of a nonlinear function of the additional state and the auxiliary input. If the uncertainties are negligible, this nonlinear function, which describes the disturbance, can be easily compensated. However, for the FLM, the state-feedback technique suffers from the uncertainties on both the motion equations and their parameters. In order to overcome this problem, the ADRC can be used to actively estimate this disturbance via ESO and compensate for it later by a feedback controller. In fact, the model of the manipulator has led to an augmented model. The last equation of this augmented model consists of the dynamics of the total disturbance, while the remaining equations represent a chain of integrators. Usually, in the classic feedback linearization technique, the function describing the disturbance is assumed to be known. For this reason, the ADRC technique is viewed as a "robust version" of the feedback linearization approach against unmodeled dynamics and parameter uncertainties. The ADRC technique has been successfully applied for different systems such as magnetic bearing systems,[14] flywheel energy storage systems[15] and control of DC motor.[16] In the context of the industry applications, a case study was presented in ref. [17] to show the advantage of ADRC over the industry standard solutions based on Proportional Intergral Derivative (PID) controller. ADRC algorithm was used by Parker Hannifin Extrusion Plant in North America in the U.S., bringing about 57% of energy saving per line across 10 production lines.[18] Texas Instrument, an industry giant, has authorized the ADRC technology in anticipation of a massive rollout of another age of control chips within which the ADRC algorithms are embedded.

Few applications of the ADRC to robotics have been reported in the literature. The ADRC was developed in ref. [19] for a flexible joint manipulator in order to limit the effects on the system caused by the nonlinear behavior. In ref. [20], the authors applied the ADRC technique to track the human gait trajectory for a lower limb rehabilitation exoskeleton. It was also applied to an selectively compliant assembly robot arm (SCARA) robot manipulator to track the desired trajectory in the joint space.[21] Compared to the feedback linearization control technique, ARDC provides smaller tracking error. In ref. [22], the ADRC was proposed for a mobile robot to track a predefined reference. Nevertheless, the ADRC strategy is not reported to be applied in the development of the FLM controllers. As mentioned, the control of FLM is challenging, due to distributed link flexibility, which makes the system non-minimum phase, under-actuated, infinite dimensional and with complex dynamics.

In this paper, an advanced version of the ADRC technique called robust ADRC is applied to FLM in order to track the desired trajectories in the joint space and to minimize the vibration of the links. The disturbances existing in the dynamics are estimated online through an ESO. Then the ADRC control law is derived using the estimated disturbance. The original version of the ARDC suffers from two major problems related to the disturbance estimation errors and parameter variations which cannot be included in the disturbances and then estimated by the extended observer. Usually, the estimation errors of the total disturbance are neglected and parameter variations of the control input are not considered. To solve such critical aspects, an advanced robust ADRC is proposed using sliding mode technique. The proposed control strategy consists of three main steps. First, an extended model is constructed from the original dynamic model of the FLM. An additional state variable that represents the total disturbances is added to the extended model. Second, the total disturbances are

https://doi.org/10.1017/S026357471900050X Published online by Cambridge University Press

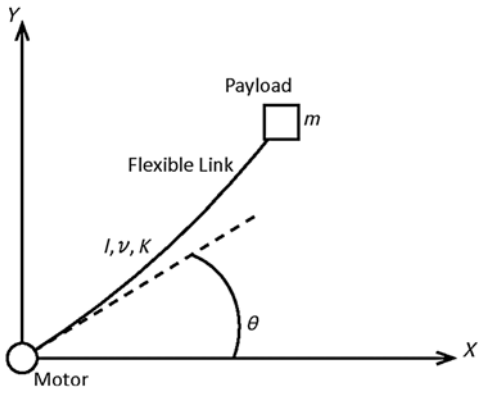

Fig. 1. Single flexible link manipulator.

estimated online through the ESO. Finally, the control law is designed to cancel the total disturbance in order to track the joint space desired trajectories and minimize link's vibration. A rigorous Lyapunov-based analysis is presented to analyze the stability of the closed loop system. The proposed ADRC control strategy is then tested on one FLM by means of numerical simulations and experiments. It has shown that the proposed ADRC has a better performance than the classic ADRC in terms of the trajectory tracking error.

The rest of the paper is organized as follows: The modeling and the description of the FLM are given in Section 2. The robust ADRC strategy is given in Section 3, which includes the ESO and control law. Section 4 presents the simulation results and discussion. The experimental results are given in Section 5. Finally, the conclusion is given in Section 6.

2. Dynamic Model of FLM

The knowledge of the dynamic model of an FLM, shown in Fig. 1, is needed for the design of the controller. A recursive Lagrangian assumed modes method has been developed by Book[23–25] to develop the mathematical model of the FLM. This method is applicable to revolute-joint robots and gives the following dynamic equations:

$$M(q)\ddot{q} + C(q, \dot{q}) + Kq = B\tau \tag{1}$$

where M and K are the positive definite inertia and stiffness matrices, respectively, $C(q, \dot{q})$ is the vector of Coriolis and centrifugal terms, q is the vector of generalized coordinates (joint positions and deflection coordinates), B is a constant matrix which depends on the shape functions used, and τ is the vector of input torques.

The deflection $y(x, t)$ of each point on link can be described as follows:[25]

$$y(x, t) = \sum_{j=1}^{m} \varphi_j(x) q_{fj}(t) \tag{2}$$

where φ_j is the jth shape function. Throughout this paper, the angle of the motor $\theta(t)$ is denoted as $q_r(t)$, the rigid part, while the flexible part is denoted as q_f. Then, the total generalized coordinate is $q = \begin{bmatrix} q_r & q_f \end{bmatrix}^T$. One FLM and only the first two modes φ_1 and φ_2 are considered in this paper. Thus, M and $K \in \Re^{3\times3}$, q and $C \in \Re^{3\times1}$, $\tau \in \Re$ and $B = \begin{bmatrix} 1 & 0 & 0 \end{bmatrix}^T$.

The model dynamics (1) has the following properties:

1. The matrix M is symmetric and positive definite.
2. The matrix $\dot{M} - 2C$ is a skew-symmetric matrix

$$\underbrace{\begin{bmatrix} I_t & M_{rf}{}^T \\ M_{rf} & M_{ff} \end{bmatrix}}_{M(q)} \underbrace{\begin{bmatrix} \ddot{q}_r \\ \ddot{q}_f \end{bmatrix}}_{\ddot{q}} + \underbrace{\begin{bmatrix} 0 & 0 \\ 0 & K_{ff} \end{bmatrix}}_{K} \underbrace{\begin{bmatrix} q_r \\ q_f \end{bmatrix}}_{q} + \underbrace{\begin{bmatrix} 2\dot{q}_r q_f^T C_{rr} \dot{q}_f \\ -\dot{q}_r^2 C_{rr} q_f \end{bmatrix}}_{C(q,\dot{q})\dot{q}} = \begin{bmatrix} 1 \\ 0 \end{bmatrix} \tau \tag{3}$$

https://doi.org/10.1017/S026357471900050X Published online by Cambridge University Press

where

$$I_t = I_M + \frac{1}{3}\rho L^3 + I_c + M_c(L + r_c)^2 : \text{ the total inertia.}$$

$$M_{rf} = \int_0^L \rho x\varphi dx + M_c\,(L + r_c)\,\varphi_L + \left(I_c + M_c r_c\,(L + r_c)\,\right)\varphi'_L : \text{ coupling term in } M$$

$$M_{ff} = \rho \int_0^L \varphi^T \varphi dx + M_c \varphi_L \varphi_L^T + \left(I_c + M_c r_c^2\right)\varphi'_L \varphi'^T_L + M_c r_c\left(\varphi'_L \varphi_L^T + \varphi_L \varphi'^T_L\right) : \text{ flexible part in } M.$$

$$C_{rr} = \rho \int_0^L \varphi^T \varphi dx + M_c \varphi_L \emptyset_L^T + M_c r_c \left(\varphi'_L \varphi_L^T + \varphi_L \varphi'^T_L\right) - \int_0^L x \int_0^x \varphi' \varphi^T ds\, dx :$$

$$-M_c\,(L + r_c) \int_0^L \varphi' \varphi'^T dx - M_c r_c L \varphi'_L \varphi'^T_L$$

$K_{ff} = EI_z \int_0^L \varphi''^T \varphi'' dx$ is the flexible part of K and $\varphi = \left[\,\varphi_1\ \varphi_2\,\right]^T$, the shape function, solution of the following equation:[25]

$$\varphi_i(x) = a_i \left[\lambda_i^3 \left(\cos\left(\frac{\lambda_i x}{L}\right) - \cosh\left(\frac{\lambda_i x}{L}\right)\right) + c_i \left(\sin\left(\frac{\lambda_i x}{L}\right) - \sinh\left(\frac{\lambda_i x}{L}\right)\right)\right] \tag{4}$$

where a_i are constants and λ_i are the solutions of the following characteristic equation:

$$det(A) = A_{11}A_{22} - A_{21}A_{12} \tag{5}$$

where

$$A_{11} = \mu_2\lambda^4(-C + Ch) + \mu_4\lambda^5(-S + Sh) + \lambda^3(-S + Sh)$$

$$A_{12} = (C + Ch) + \mu_2\lambda(-S + Sh) + \mu_2\lambda^2(-C + Ch)$$

$$A_{21} = -\,(\mu_1 + \mu_5)\,\lambda^6(S + Sh) + \lambda^3(C + Ch) + \mu_4\lambda^5(C - Ch)$$

$$A_{22} = (S + Sh) + (\mu_1 + \mu_5)\,\lambda^3(C - Ch) + \mu_4\lambda^2(S - Sh)$$

$$\text{and } \mu_1 = \frac{I_c}{\rho L^3},\ \mu_2 = \frac{M_c}{\rho L},\ \mu_4 = \frac{M_c r_c}{\rho L^2},\ \mu_5 = \frac{M_c r_c^2}{\rho L^3} \text{et } \lambda = \beta L$$

$C = \cos\lambda$, $S = \sin\lambda$, $Ch = \cosh\lambda$ et $Sh = \sinh\lambda$

L is the length of the flexible link.

φ_L is the shape function defined at the extremity of the link, ρ is the mass density, L is the link length, M_c is the tip mass and r_c is the payload center of mass.

3. Robust ADRC for FLM

The FLM is an under-actuated, non-minimum phase and highly nonlinear system which makes its control a challenging task. The model-based approach is dependent on the accuracy of the mathematical model, while the standard PID or any model-free approach has limitations in dealing with problems with disturbances. Our goal is to develop a robust controller based on the ADRC technique that is capable to estimate unknown knowledge of the manipulator and eliminate its effect in the control law in order to achieve a good tracking of the desired trajectory and to minimize the link's vibration.

The dynamical equations of the robot can be viewed as two interconnected subsystems, rigid and flexible part, as follows:

$$\begin{bmatrix} M_r & M_{rf} \\ M_{fr} & M_f \end{bmatrix} \begin{bmatrix} \ddot{q}_r \\ \ddot{q}_f \end{bmatrix} + \begin{bmatrix} C_r(q, \dot{q}) \\ C_f(q, \dot{q}) \end{bmatrix} + \begin{bmatrix} 0 & 0 \\ 0 & K_f \end{bmatrix} \begin{bmatrix} q_r \\ q_f \end{bmatrix} = \begin{bmatrix} 1 \\ 0 \end{bmatrix} \tau \tag{6}$$

https://doi.org/10.1017/S026357471900050X Published online by Cambridge University Press

The dynamic model (6) can be written in terms of two equations:

$$M_r\ddot{q}_r + M_{rf}\ddot{q}_f + C_r = \tau \tag{7}$$

$$M_{fr}\ddot{q}_r + M_f\ddot{q}_f + C_f + K_{ff}q_f = 0 \tag{8}$$

From Eq. (8), $\ddot{q}_f$ can be expressed as follows:

$$\ddot{q}_f = -M_f^{-1}\left[M_{fr}\ddot{q}_r + C_f + K_f q_f\right] \tag{9}$$

Inserting Eq. (9) in Eq. (7), the dynamic model can be written as

$$M_r^*\ddot{q}_r + C_r^* + K_f^* q_f = \tau \tag{10}$$

where $M_r^* = M_r - M_{rf}M_f^{-1}M_{fr}$; $C_r^* = C_r - M_{rf}M_f^{-1}C_f$; $K_f^* = -M_{rf}M_f^{-1}K_f$.

The ADRC approach unfolds into three main steps: (1) construction of an extended model from the original dynamic model. The extended model includes an additional state variable representing the external disturbances and nonlinearities. (2) Estimation of the states using ESO. (3) The design of the control law that tracks the desired trajectories and to minimize the link's vibration.

3.1. Extended model for FLM

The extended model is obtained from the final equation of motion (10), where the input is the torque τ and the output is the generalized coordinate q. Equation (10) can be expressed as

$$\ddot{q}_r = -M_r^{*-1}\left(C_r^* + K_f^* q_f\right) + M_r^{*-1}\tau \tag{11}$$

By defining the state variables $x_1 = q_r$ and $x_2 = \dot{q}_r$, the state space model can be written as follows:

$$\begin{cases} \dot{x}_1 = x_2 \\ \dot{x}_2 = f + bu \end{cases} \tag{12}$$

where $f = -M_r^{*-1}\left(C_r^* + K_f^* q_f\right)$; $b = M_r^{*-1}$ and $u = \tau$. Let us define an extra state, representing the total disturbance $x_3 = f$, the augmented state space is given as follows:

$$\begin{cases} \dot{x}_1 = x_2 \\ \dot{x}_2 = x_3 + bu \\ \dot{x}_3 = h \end{cases} \tag{13}$$

where $h = \dot{f}$.

Note that the objective of the ADRC technique is to obtain proper estimation, to minimize the total disturbance and to obtain a good trajectory tracking. The traditional ADRC control law is given by[12]

$$u = \frac{1}{\hat{b}}(-\hat{x}_3 + u_0) \tag{14}$$

where u_0 is the auxiliary control variables given from a feedback controller. $\hat{x}_3$ is the estimate of x_3. The type of controller in ADRC should ensure the closed loop stability of the system.

The estimation of the total disturbance f (namely $\hat{x}_3$) is obtained via the ESO technique.

Note that the model (13) is an extended dynamic model. This extended model is used to estimate the total disturbance f. Model (12) represents a different way to describe the model (11) as well as the original models (6) and (1). This transformation to the extended model is required to linearize the model of the FLMs using a state feedback approach. The theory of the feedback linearization for nonlinear system transforms the nonlinear behavior to chain of integrators. Unfortunately, this technique is sensitive to the parameter variations. In order to overcome this limitation, the authors propose a robust controller to deal with the parameter uncertainties and the torque disturbances by using sliding mode technique in the control law.

https://doi.org/10.1017/S026357471900050X Published online by Cambridge University Press

3.2. ESO for FLM

The ESO of extended model is used to estimate the total disturbance f. With u and x_1 as inputs, the ESO is given as follows:

$$\begin{cases} \dot{\hat{x}}_1 = \hat{x}_2 - g_1(e_1) \\ \dot{\hat{x}}_2 = \hat{x}_3 - g_2(e_1) + bu \\ \dot{\hat{x}}_3 = -g_3(e_1) \end{cases} \tag{15}$$

where $e_1 = \hat{x}_1 - x_1$ is the estimation errors; $g_i(.)$ $i = 1, 2, 3$, is chosen to be linear or nonlinear function. The error dynamics can be described as follows:

$$\begin{cases} \dot{e}_1 = \dot{\hat{x}}_1 - \dot{x}_1 = \hat{x}_2 - g_1(e_1) - x_2 = e_2 - g_1(e_1) \\ \dot{e}_2 = \dot{\hat{x}}_2 - \dot{x}_2 = \hat{x}_3 - g_2(e_1) + bu - x_3 - bu = e_3 - g_2(e_1) \\ \dot{e}_3 = \dot{\hat{x}}_3 - \dot{x}_3 = -g_3(e_1) - \dot{f} \end{cases} \tag{16}$$

In this paper, we focus on linear ESO, that is, $g_i(e_1) = \alpha_i e_1$, where $i = 1, 2, 3$. α_i is a positive constant. The error dynamics (16) can be expressed in the following state space:

$$\begin{cases} \dot{e}_1 = e_2 - \alpha_1 e_1 \\ \dot{e}_2 = e_3 - \alpha_2 e_1 \\ \dot{e}_3 = -\dot{f} - \alpha_3 e_1 \end{cases} \tag{17}$$

In a compact form, Eq. (17) can be given as follows:

$$\dot{e} = Ae + B\dot{f} \tag{18}$$

where $A = \begin{bmatrix} -\alpha_1 & 1 & 0 \\ -\alpha_2 & 0 & 1 \\ -\alpha_3 & 0 & 0 \end{bmatrix}$ and $B = \begin{bmatrix} 0 \\ 0 \\ -1 \end{bmatrix}$.

Assuming that $\dot{f}$ is bounded $\left|\dot{f}\right| \leq M_f$ and A is a Hurwitz matrix, the error dynamics is exponentially stable.[26]

For the purpose of tuning simplification, all the observer poles are placed at $-\omega_0$. The parameter α_i is computed such that the matrix A is Hurwitz, that is, the real part of the eigenvalues of A is negative. The observer gains can be determined according to the characteristic polynomial.[12]

$$s^3 + \alpha_1 s^2 + \alpha_2 s + \alpha_3 = (s + \omega_0)^3 \tag{19}$$

where ω_0 is the observer bandwidth and $\alpha = \begin{bmatrix} 3\omega_0 & 3\omega_0^2 & \omega_0^3 \end{bmatrix}^T$.

The observer bandwidth should properly be selected in a trade-off between the tracking performance and the noise tolerance, because a larger observer bandwidth increases the accuracy of the estimation and at the same time will increase noise sensitivity. The simulation results are given in Section 4 for different values of ω_0 in order to select the best value to be used for the ADRC.

3.3. Design of the control law

One ideal candidate in the control theory is the ADRC, which has a very good disturbance rejection capability. Both the internal dynamics and the external disturbances can be estimated and compensated in real time. Unfortunately, two major limits have to be addressed in order to improve the robustness of the ADRC technique. First, the occurrence of estimated error of the total disturbance f, which can harm the performance of the ADRC. The second limit is related to the uncertainty of the systems parameters in the control gains $b = M_r^{*-1}$. To the best of the authors' knowledge, these issues have not been addressed previously for robotics systems.

For the first problem, the estimation error can occur because the estimate of the disturbances $\hat{x}_3$ is based on the rigid and flexible generalized coordinate q, which is affected by uncertainties. This uncertainty is due to the fact that the estimation of the disturbances depends on the position of the velocity of the rigid and flexible parts and both of these signals are affected by uncertainties. Indeed, the velocity measurement $\dot{q}$ is corrupted by noise and the position q, which is estimated by

https://doi.org/10.1017/S026357471900050X Published online by Cambridge University Press

an observer depending on the correctness of the adopted rigid and flexible generalized coordinate. As a conclusion, the estimate of the ESOs will be affected by errors, because these signals are affected by errors. As shown in (18), the convergence of the ESO is not related to the model parameter, which confirms the robustness of the ESO. However, the rigid coordinate x_1, represents the measured signal and if it is affected by errors, for sure $\hat{x}_1$ will not converge to the true value. Since x_2 and x_3 are derived from x_1 and $\hat{x}_1$, they will also be affected by error. In addition, the parameter b appears in the control gain (12), which depends on the inertia that can vary when the load is either mounted or disconnected. Thus, the parameter b is affected by uncertainties that cannot be included in the disturbance and consequently cannot by estimated by ESO.

It is possible to estimate the disturbance f, namely x_3, using the extended model (13). Let us consider the parameter b affected by uncertainties and it varies between a minimum value b_m and a maximum value b_M, that is, $b \in [b_m, b_M]$ and the rated (nominal) value is $\hat{b} = \sqrt{b_m b_M}$.[27] Using the extended model (13) and the control input (14), the controlled model becomes

$$\begin{cases} \dot{x}_1 = x_2 \\ \dot{x}_2 = f - \frac{b}{\hat{b}}\hat{x}_3 + \frac{b}{\hat{b}}u_0 \end{cases} \tag{20}$$

Equation (20) is equivalent to

$$\begin{cases} \dot{x}_1 = x_2 \\ \dot{x}_2 = \eta + \frac{b}{\hat{b}}u_0 \end{cases} \tag{21}$$

where $\eta = f - \frac{b}{\hat{b}}\hat{x}_3$ is the new disturbance.

The knowledge of $\frac{b}{\hat{b}}$ is required in order to estimate η via ESO technique. Since $\frac{b}{\hat{b}}$ is unknown, the disturbance η cannot be compensated. In order to overcome the two aforementioned issues, consider the following assumption that is useful for the development of the new control law based on sliding mode control.

A1. The estimation error of the total disturbance $\hat{x}_3 = \hat{f}$ is bounded:

$$\left|\tilde{f}\right| \leq \varepsilon \hat{f} \tag{22}$$

where $\tilde{f} = f - \hat{f}$

A2. The parameter b is uncertain and varies between its minimum and maximum values b_m and b_M, such that

$$\frac{1}{\beta} \leq \frac{b}{\hat{b}} \leq \beta \tag{23}$$

where $\hat{b} = \sqrt{b_m b_M}$ and $\beta = \sqrt{b_M / b_m}$.

The proposed control law is given as follows:

$$\tau = u = \frac{1}{\hat{b}}\left[-\beta^{-1}(\varepsilon + 1)\hat{f} + u_0 + \lambda\dot{\tilde{q}}_r - K_s \operatorname{sign}(s)\right] \tag{24}$$

where $u_0 = \beta^{-1}\left(\ddot{q}_{rd} - \lambda\dot{\tilde{q}}_r + (\beta - 1)K_s \operatorname{sign}(s)\right)$; $s = \dot{\tilde{q}}_r + \lambda\tilde{q}_r$; $\tilde{q}_r = q_r - q_{rd}$ and K_s is positive parameter gain.

Remark 1. Note that, in the traditional ADRC, the estimation errors and the uncertainties in the control gain b are not considered ($f = \hat{f}$ and $b = \hat{b}$). In the proposal robust control strategy, we can easily switch to the traditional ADRC by using $f - \hat{f} = 0$, $\beta = 1$ ($b_m = b_M$, *i.e.*, $b = \hat{b}$) and $K_s = 0$.

For the stability analysis, let us propose the following Lyapunov function:

$$V(t) = \frac{1}{2}s^2 \tag{25}$$

https://doi.org/10.1017/S026357471900050X Published online by Cambridge University Press

Take the time derivative of V to get

$$\begin{aligned}
\dot{V}(t) &= s\dot{s} \\
&= s\left(\dddot{\tilde{q}}_r + \lambda\ddot{\tilde{q}}_r\right) \\
&= s\left(\dddot{q}_r - \dddot{q}_{rd} + \lambda\ddot{\tilde{q}}_r\right) \\
&= s\left(-\dddot{q}_{rd} + f + bu + \lambda\ddot{\tilde{q}}_r\right) \\
&= s\left(-\dddot{q}_{rd} + \lambda\ddot{\tilde{q}}_r + f + \frac{b}{\hat{b}}\left[-\left(\beta^{-1} + \varepsilon\beta^{-1}\right)\hat{f} + u_0 - K_s\,\mathrm{sign}(s)\right]\right) \\
&= s\left(-\dddot{q}_{rd} + \lambda\ddot{\tilde{q}}_r + \tilde{f} + \hat{f} + \frac{b}{\hat{b}}\left[-\left(\beta^{-1} + \varepsilon\beta^{-1}\right)\hat{f} + u_0 - K_s\,\mathrm{sign}(s)\right]\right) \\
&= s\left(-\dddot{q}_{rd} + \lambda\ddot{\tilde{q}}_r + \tilde{f} + \hat{f} - \frac{b}{\hat{b}}\left(\beta^{-1} + \varepsilon\beta^{-1}\right)\hat{f} + \frac{b}{\hat{b}}\left[u_0 - K_s\,\mathrm{sign}(s)\right]\right) \\
&= s\left(-\dddot{q}_{rd} + \lambda\ddot{\tilde{q}}_r + \tilde{f} + \hat{f} - \frac{b}{\hat{b}}\left(\beta^{-1} + \varepsilon\beta^{-1}\right)\hat{f} + \frac{b}{\hat{b}}\beta^{-1}\ddot{q}_{rd} - \frac{b}{\hat{b}}\beta^{-1}\lambda\ddot{\tilde{q}}_r\right. \\
&\qquad \left. + \frac{b}{\hat{b}}\beta^{-1}(\beta-1)\,K_s\,sign\,(s) - \frac{b}{\hat{b}}\left[K_s\,\mathrm{sign}(s)\right]\right) \\
&= s\left(-\dddot{q}_{rd} + \lambda\ddot{\tilde{q}}_r + \tilde{f} + \hat{f} - \frac{b}{\hat{b}}\left(\beta^{-1} + \varepsilon\beta^{-1}\right)\hat{f} + \frac{b}{\hat{b}}\beta^{-1}\ddot{q}_{rd} - \frac{b}{\hat{b}}\beta^{-1}\lambda\ddot{\tilde{q}}_r - \frac{b}{\hat{b}}\beta^{-1}K_s\,\mathrm{sign}\,(s)\right) \\
&= \frac{b}{\hat{b}}\beta^{-1}s\left(\left[-\ddot{q}_{rd} + \lambda\ddot{\tilde{q}}_r + (1+\varepsilon)\hat{f}\right]\left(\frac{b}{\hat{b}}\beta^{-1}\right)^{-1} - (1+\varepsilon)\hat{f} + \ddot{q}_{rd} - \lambda\ddot{\tilde{q}}_r - K_s\mathrm{sign}\,(s)\right) \\
&= \frac{b}{\hat{b}}\beta^{-1}s\left(\left[-\ddot{q}_{rd} + \lambda\ddot{\tilde{q}}_r + (1+\varepsilon)\hat{f}\right]\left(\beta\left(\frac{b}{\hat{b}}\right)^{-1} - 1\right) - K_s\,\mathrm{sign}\,(s)\right)
\end{aligned}$$

For a system to be stable, the outputs should be bounded; that is, $|\dddot{q}_{rd}| < Q_d$, $\left|\ddot{\tilde{q}}_r\right| < \psi_r$, $|s| \le S$ and $\left|\hat{f}\right| < F$, where Q_d, ψ_r and F are some positive values. Defining K_s to be $K_s = \frac{b}{\hat{b}}\beta^{-1}$, $\dot{V}(t)$ becomes,

$$\dot{V}(t) \le \left|1 - \frac{b}{\hat{b}}\beta^{-1}\right| |s|\left(|\dddot{q}_{rd}| + \lambda\left|\ddot{\tilde{q}}_r\right| + (1+\varepsilon)\left|\hat{f}\right|\right) - K_s$$

If K_s is chosen to be large enough such as

$$\left|1 - \frac{b}{\hat{b}}\beta^{-1}\right| S\,(Q_d + \lambda\psi_r + (1+\varepsilon)\,F) \le K_s \tag{26}$$

Then, $\dot{V}$ becomes

$$\dot{V}(t) \le 0 \tag{27}$$

Using Eq. (26), we can conclude that the time derivative of $V(t)$ is negative. By Eq. (27), V is monotonously decreasing. Therefore, $s \in L_\infty$. According to the definition of the sliding surface s after Eq. (24), we know that $\tilde{q}_r$ and $\dot{\tilde{q}}_r$ are bounded and uniformly continuous. Then using Barbalat lemma,[27] we can conclude that the closed loop system is asymptotically stable.

4. Simulation Results

The proposed ADRC for FLM is shown in Fig. 2. The ESO is used to estimate existing disturbances for the joint and the flexible link, where q_d is the desired trajectory of the rigid and flexible link. The outputs of the ESO are $\hat{q}$ and $\dot{\hat{q}}$, while τ_0 is the output of the ADRC. Two simulations are carried out

https://doi.org/10.1017/S026357471900050X Published online by Cambridge University Press

Table I. Nominal parameters.

Parameters	**Nominal value**
Motor inertia (I_m)	0.02 kg m^2
Beam length (L)	1 m
Beam linear density (ρ)	0.62 kg/m
Beam rigidity (EI_z)	12.85 N m^2
Payload mass (M_c)	0.3 kg
Payload inertia (I_c)	0 kg m^2
Payload center of mass (r_c)	0 m

Table II. Root mean square error between desired and measured states for different ω_0 values when $f = \hat{f}$ and $b = \hat{b}$.

	$\sqrt{\frac{\sum\left(q_{i_{desired}} - q_{i_{measured}}\right)^2}{n}} \times 10^3$ **in rad for** ω_0**=**												
q_i	**0–20**	**150**	**160**	**170**	**180**	**190**	**200**	**210**	**220**	**230**	**240**	**250**	**260**
q_r	No Tracking	183.2	183.2	183.1	183.1	183.1	183.0	183.0	183.0	182.9	182.9	182.8	1267.7
q_{f_1}		8.7	8.7	8.7	8.6	8.6	8.5	8.5	8.5	8.5	8.5	8.4	64.5
q_{f_2}		0.2	0.2	0.2	0.2	0.2	0.2	0.2	0.2	0.2	0.2	0.2	1.4

Table III. Root mean square error between estimated and measured states for different ω_0 values when $f = \hat{f}$ and $b = \hat{b}$.

	$\sqrt{\frac{\sum\left(q_{i_{estimated}} - q_{i_{measured}}\right)^2}{n}}$ **in rad for** $\omega_0 =$												
q_i	**0**	**150**	**160**	**170**	**180**	**190**	**200**	**210**	**220**	**230**	**240**	**250**	**260**
q_r	No Tracking	31 $\times 10^{-6}$	24 $\times 10^{-6}$	19 $\times 10^{-6}$	15 $\times 10^{-6}$	12 $\times 10^{-6}$	5.3 $\times 10^{-6}$	12 $\times 10^{-6}$	7 $\times 10^{-6}$	5.1 $\times 10^{-6}$	3.5 $\times 10^{-6}$	1.1 $\times 10^{-6}$	0.28

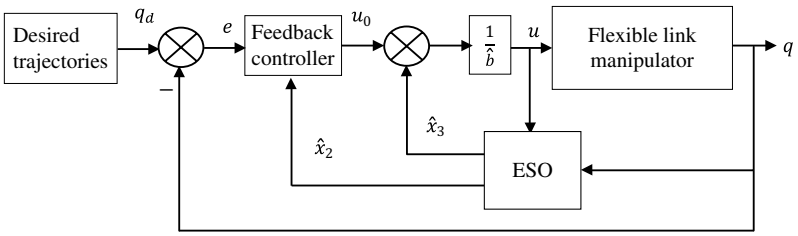

Fig. 2. Block diagram of the ADRC technique.

in MATLAB/Simulink, one without estimation errors and uncertainties in the control gain b ($f = \hat{f}$ and $b = \hat{b}$) and the other when $f \neq \hat{f}$ and $b \neq \hat{b}$. The external disturbance is generated randomly by using the function "randn" in MATLAB. The ESO can estimate the system state and the "total disturbance" in real time based on the ADRC. The choice of the bandwidth ω_0 has a significant effect on the tracking performance. This effect can be observed on the convergence rate between the real states and the estimated states, and the overall performance can be observed as the system states converge to the desired states. The nominal values of one FLM are given in Table I and Figure 3, Tables II and III describe the system performance when $f = \hat{f}$ and $b = \hat{b}$.

https://doi.org/10.1017/S026357471900050X Published online by Cambridge University Press

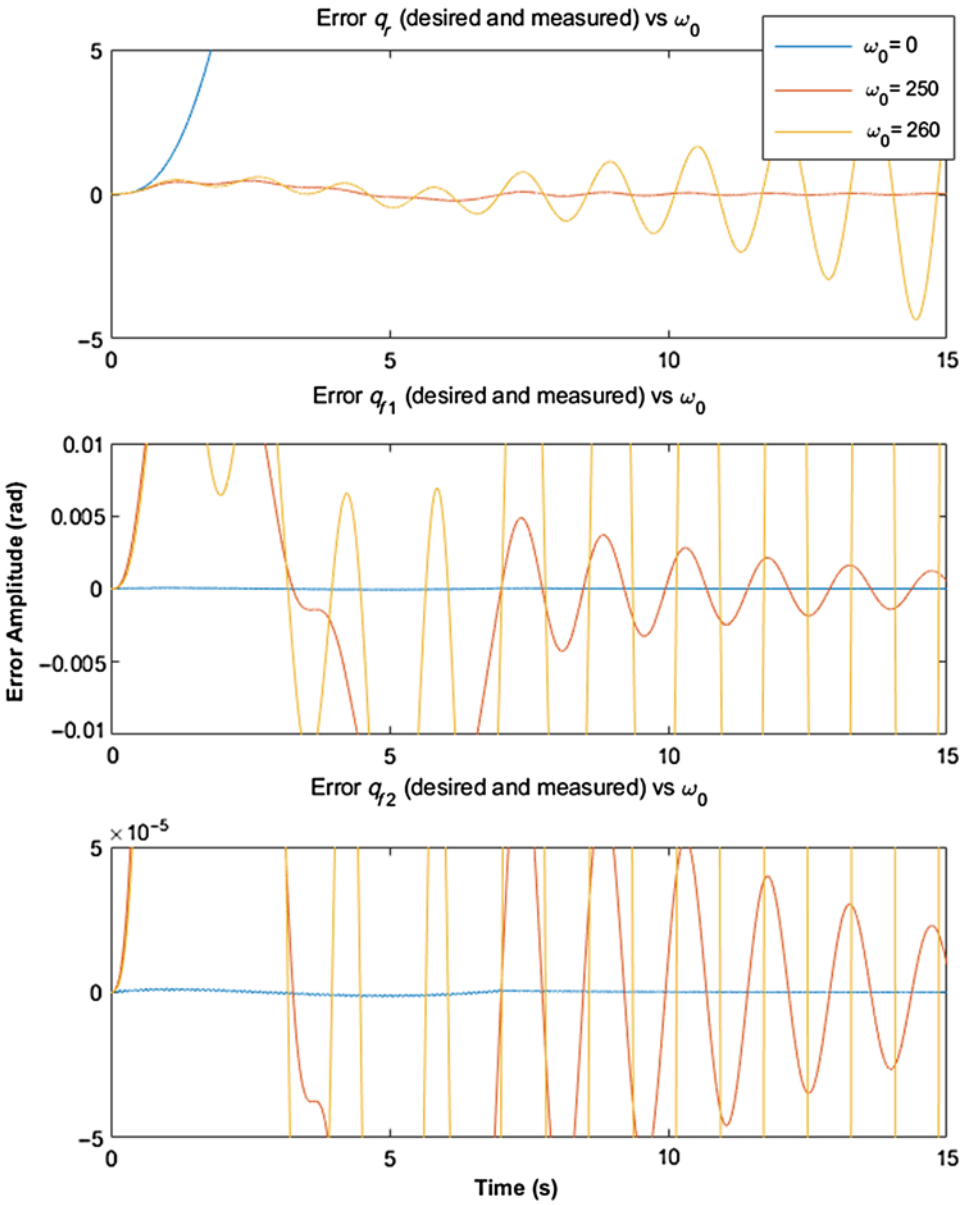

Fig. 3. The effect of ω_0 on the performance of the controller when $f = \hat{f}$ and $b = \hat{b}$.

Tables II, III and Fig. 3 show that for very small value of ω_0, $\omega_0 < 100$, the estimated states converged slowly toward the measured states, and the overall performance was smooth but with high error values. When the value of ω_0 increased, the estimated states started to converge faster toward the measured states, and the overall performance became better as the error became smaller. After increasing the values of ω_0 above certain limit $\omega_0 > 260$, the convergence rate between the estimated states and the measured states became faster and faster. However, the error started to increase and chattering was observed. The reason of this is that the system becomes more sensitive to the noise and uncertainties. Therefore, the value of ω_0 should be chosen carefully; large value results in fast convergence with chattering and more sensitivity to uncertainties, and low value results in smooth performance with slow convergence and more error. According to the results, the best value of $\omega_0 = 250$.

Now after fixing the value of $\omega_0 = 250$, let check the performance of the controller. Two cases are studied here. First, without estimation errors in f or uncertainties in the control gain b, that is,

https://doi.org/10.1017/S026357471900050X Published online by Cambridge University Press

Table IV. Root mean square error between desired and measured states for different K_s values, when $f = \hat{f}$ and $b = \hat{b}$.

	$\sqrt{\frac{\sum(q_{i_{desired}} - q_{i_{measured}})^2}{n}}$ in μrad for K_s =											
q_i	**0.010**	**0.012**	**0.014**	**0.016**	**0.018**	**0.020**	**0.022**	**0.024**	**0.026**	**0.194**	**0.196**	**0.198**
q_r	35.48	35.53	35.49	35.49	35.25	35.39	35.56	35.35	35.60	51.78	50.02	49.91
q_{f_1}	77.74	77.74	77.75	77.78	77.88	77.80	77.81	77.80	77.89	84.15	84.45	85.07
q_{f_2}	1.640	1.650	1.650	1.660	1.660	1.660	1.680	1.670	1.680	3.410	3.180	3.330

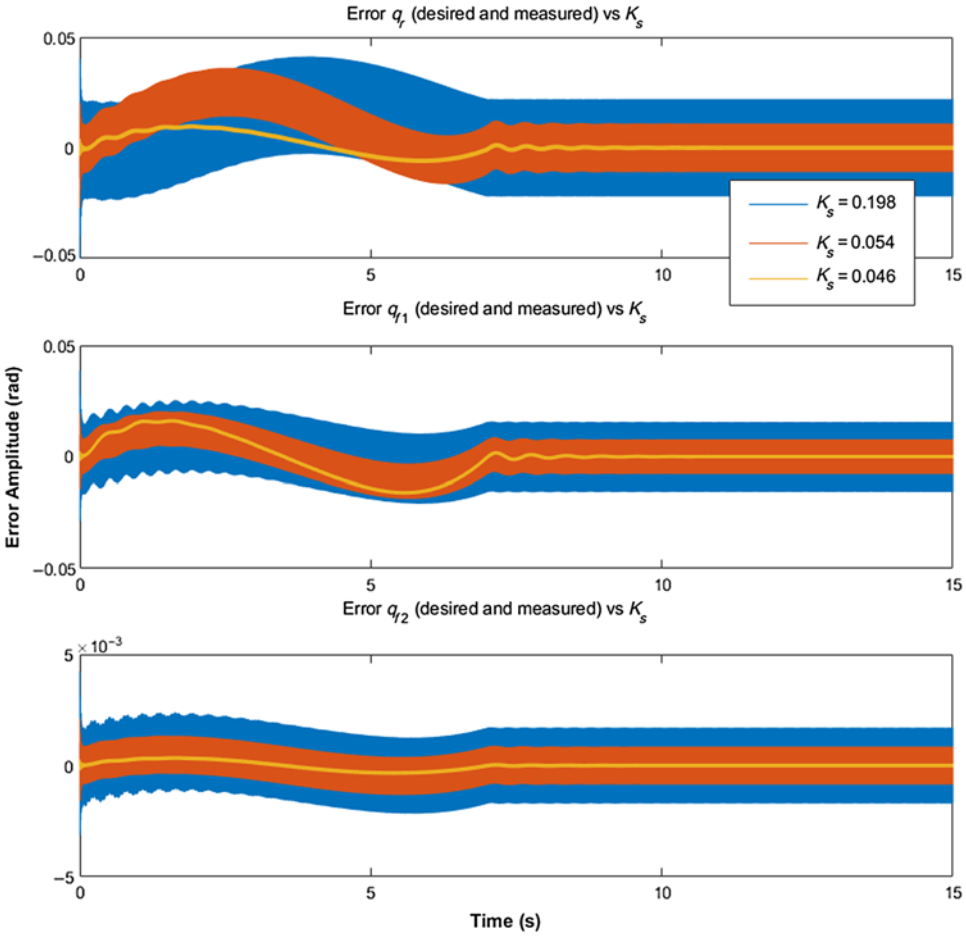

Fig. 4. The effect of K_s on the performance of the controller when $f = \hat{f}$ and $b = \hat{b}$.

the values of $\hat{f}$ and $\hat{b}$ are equal to their actual values f and b, respectively. Second, when we have estimation errors in f and uncertainties in the control gain b ($f \neq \hat{f}$ and $b \neq \hat{b}$).

The simulation results for the first case when $f = \hat{f}$ and $b = \hat{b}$ are given in Table IV and Figs. 4–7. Table IV shows the root mean square error (RMSE) between desired and measured states for different K_s values to select the best value. Figure 4 presents the tracking error for rigid and flexible coordinate for three different values of K_s (0.002, 0.018 and 0.198) to show the performance of the controller.

Figure 4 and Table IV show the effect of the discontinuous gain on the system when estimation errors or uncertainties are negligible. It is obvious that when increasing the gain, the system

https://doi.org/10.1017/S026357471900050X Published online by Cambridge University Press

Table V. The comparison between the proposed robust ADRC and the traditional ADRC, when $f = \hat{f}$ and $b = \hat{b}$.

	Robust ADRC					**Traditional ADRC**				
	MAE (rad)	**RMSE (rad)**	**OS (%)**	**ST (s)**	**|SSE| (rad)**	**MAE (rad)**	**RMSE (rad)**	**OS (%)**	**ST (s)**	**|SSE| (rad)**
q_r	9×10^{-3}	4×10^{-5}	0.0	6.02	2×10^{-4}	0.9	5×10^{-1}	0.1	6.4	3×10^{-5}
q_{f_1}	1.7×10^{-2}	7×10^{-5}	–	–	1×10^{-4}	6×10^{-2}	1×10^{-2}	–	–	2×10^{-5}
q_{f_2}	4×10^{-4}	1.7×10^{-6}	–	–	3×10^{-5}	1×10^{-3}	2×10^{-4}	–	–	1×10^{-7}

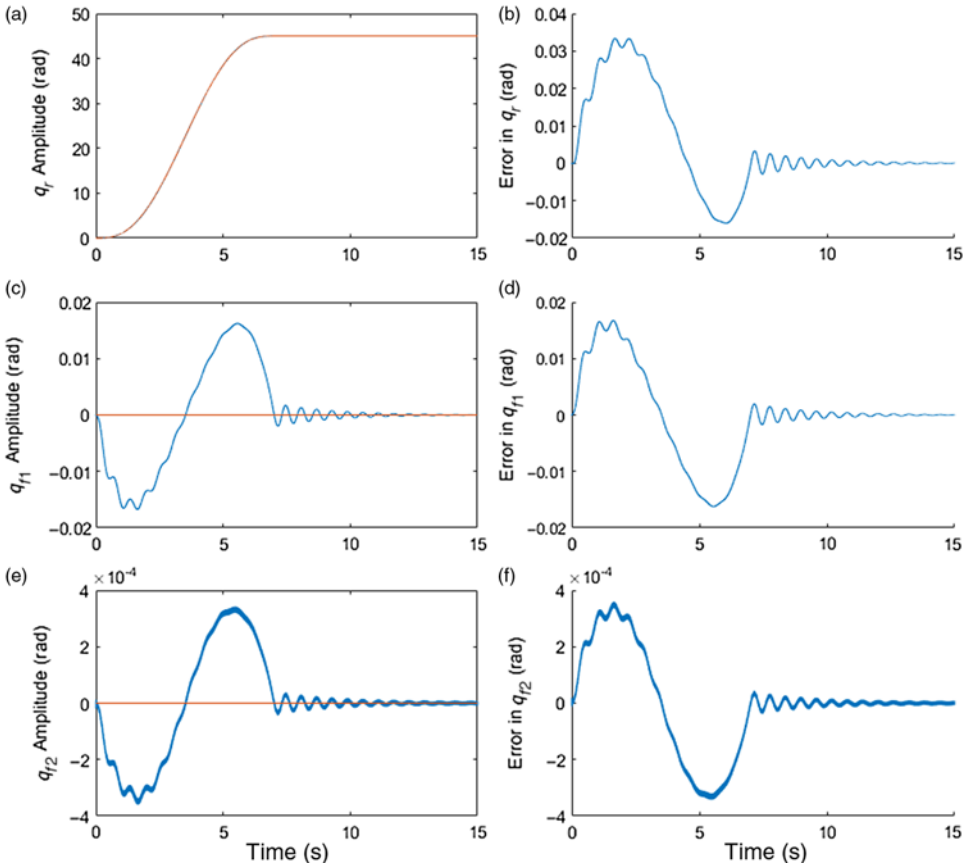

Fig. 5. The performance of the proposed robust controller when $f = \hat{f}$ and $b = \hat{b}$: (a) is the state q_r desired versus measured, (b) the error in q_r, (c) is the state q_{f1} desired versus measured, (d) the error in q_{f1}, (e) is the state q_{f2} desired versus measured and (f) the error in q_{f2}.

becomes more stable and the errors are reduced (up to K_s = 0.018). However, chattering presents where the response oscillates several times and the system vibrates. Keep increasing the gain, the system performance become worse and its stability is affected.

The proposed robust control strategy is compared with the traditional ADRC. The simulation results with the traditional ADRC are given in Fig. 6.

Table V shows the comparison between the proposed robust ADRC and the traditional ADRC in terms of maximum absolute error (MAE) obtained, the RMSE, the overshoot (OS), the settling time (ST) and the steady state error (SSE).

Figures 5 and 6 and Table V show a comparison between the proposed robust ADRC, with K_s value = 0.018, and the traditional ADRC. Now, let us move to the case when the estimation error

https://doi.org/10.1017/S026357471900050X Published online by Cambridge University Press

Table VI. The parameters of the proposed robust ADRC, when $f \neq \hat{f}$ and $b \neq \hat{b}$.

	Robust ADRC				
	MAE (rad)	**RMSE (rad)**	**OS (%)**	**ST (s)**	**|SSE| (rad)**
q_r	7×10^{-3}	4×10^{-5}	0.0	6.02	2×10^{-5}
q_{f_1}	1.6×10^{-2}	7×10^{-5}	–	–	8×10^{-4}
q_{f_2}	3×10^{-4}	1.7×10^{-6}	–	–	4×10^{-5}

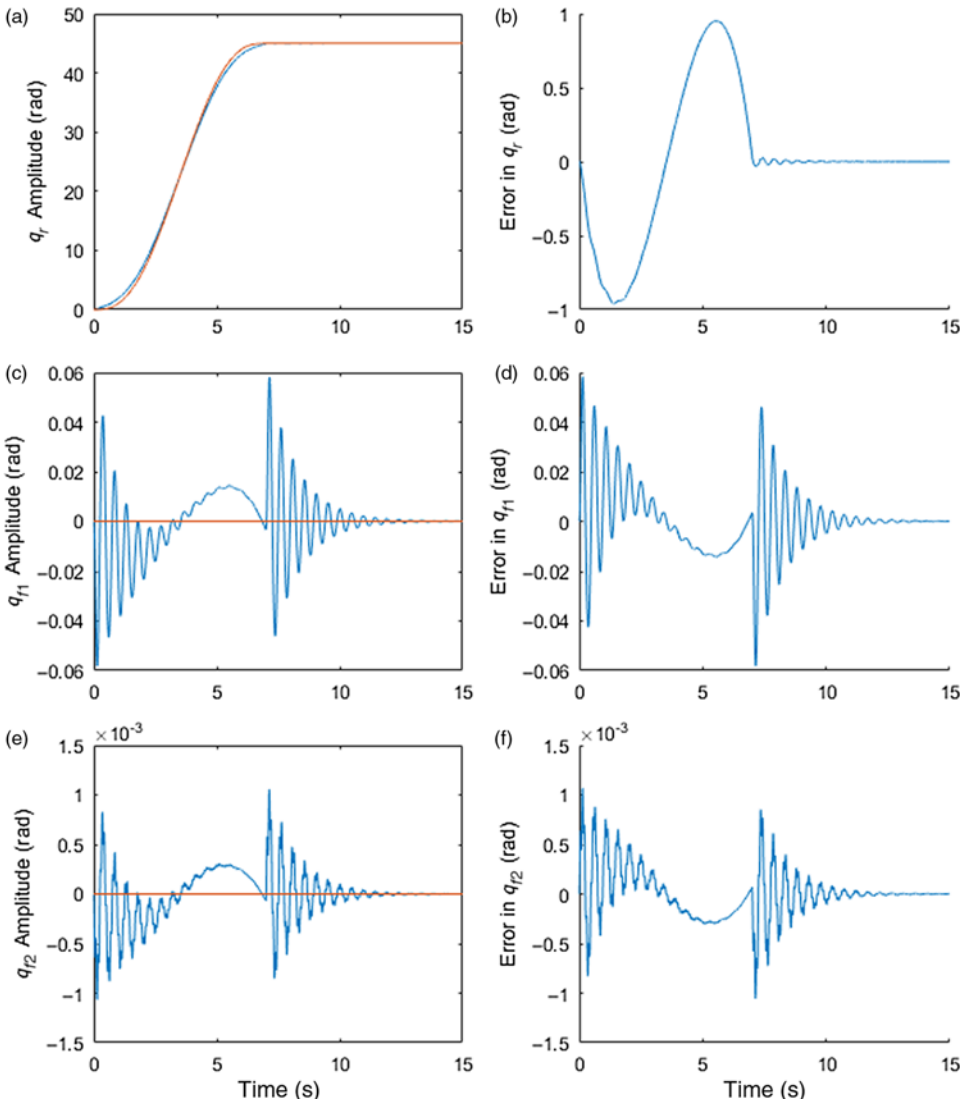

Fig. 6. The performance of the ADRC when $f = \hat{f}$ and $b = \hat{b}$: (a) is the state q_r desired versus measured, (b) the error in q_r, (c) is the state q_{f1} desired versus measured, (d) the error in q_{f1}, (e) is the state q_{f2} desired versus measured and (f) the error in q_{f2}.

of f and the uncertainties in b are considered as $f \neq \hat{f}$ and $b \neq \hat{b}$, respectively. The simulations are done with $\varepsilon = 1$; $b_M = 10$; $b_m = 5 \times 10^{-3}$; $\lambda = 0.1$ and $K_s = 0.018$. Figure 7 shows the tracking trajectories as well as their tracking errors. Table VI shows the MAE, RMSE, OS, ST, and SSE for the proposed controller when $f \neq \hat{f}$ and $b \neq \hat{b}$.

https://doi.org/10.1017/S026357471900050X Published online by Cambridge University Press

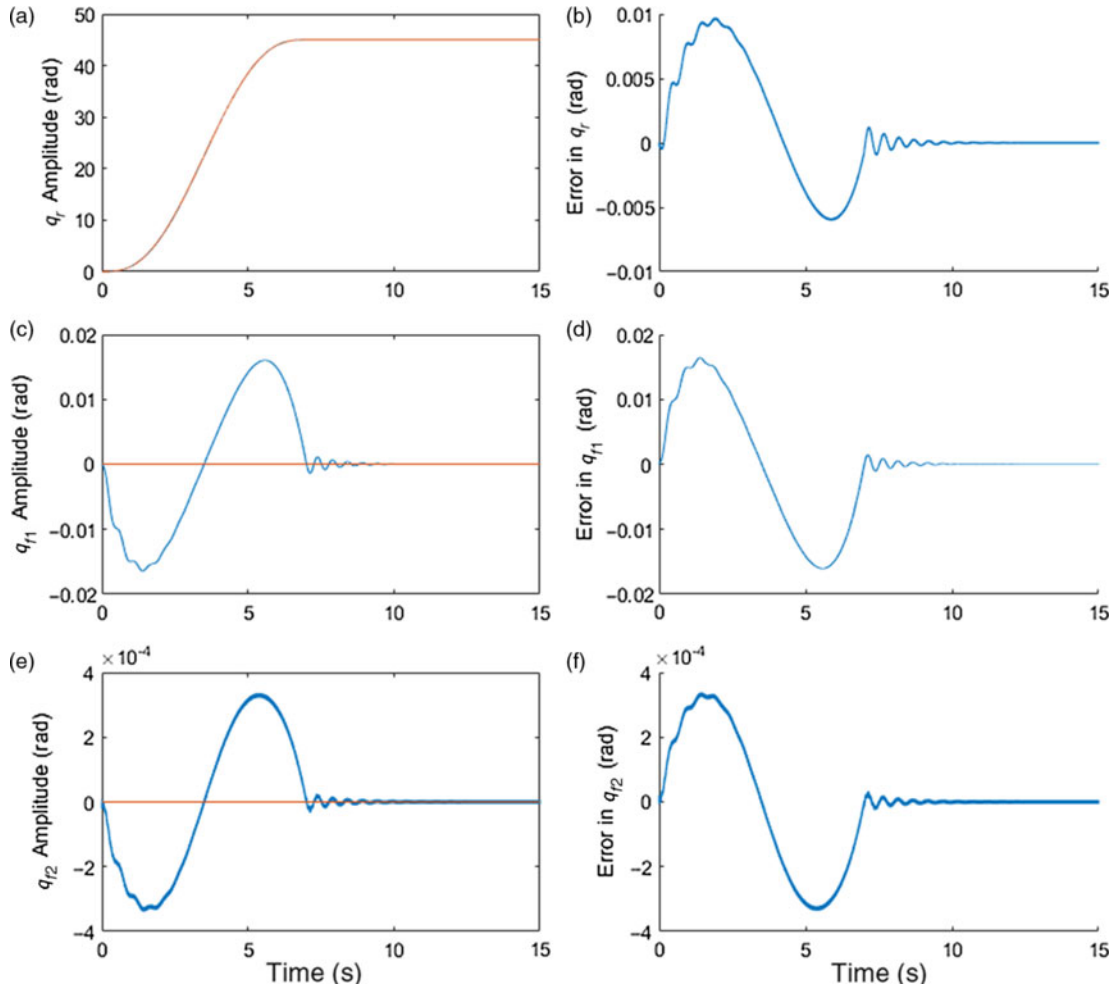

Fig. 7. The performance of the proposed robust controller when $f \neq \hat{f}$ and $b \neq \hat{b}$.

Figures 5 and 6 and Table V show a comparison between the proposed controller and the traditional ARDC. It has been found that the robust ADRC has a superior performance compared to traditional ADRC in terms of MAE, RMSE, OS, and ST. On the other hand, traditional ADRC has a lower SSE compared to the proposed robust ADRC, and that occurs because the robust ADRC has the discontinuous gain, which causes a chattering around the final value.

After injecting uncertainties in the system; that is, $f \neq \hat{f}$ and $b \neq \hat{b}$, the performance was monitored by Fig. 7 and Table VI. They show that the performance will not be affected that much. However, chattering is reduced and therefore the errors become smaller.

The proposed ADRC is compared with a well-known computed torque approach[28] using the following control law:

$$\tau = M_r^* u + C_r^* + K_f^* q_f \tag{28}$$

where $u = \ddot{q}_r + K_{dc}\dot{\tilde{q}}_r + K_{pc}\tilde{q}_r$. $\tilde{q}_r = q_r - q_{rd}$; K_{dc} and K_{pc} are positive parameters gains.

The simulation results using the computed torque approach are given in Fig. 8. The parameters used for the computed torque approach are K_{pc} = 80 and K_{dc} = 20. The simulation results using computed torque technique show a good tracking but with tracking errors higher than the proposed ADRC technique, which prove the effectiveness of the ADRC approach.

https://doi.org/10.1017/S026357471900050X Published online by Cambridge University Press

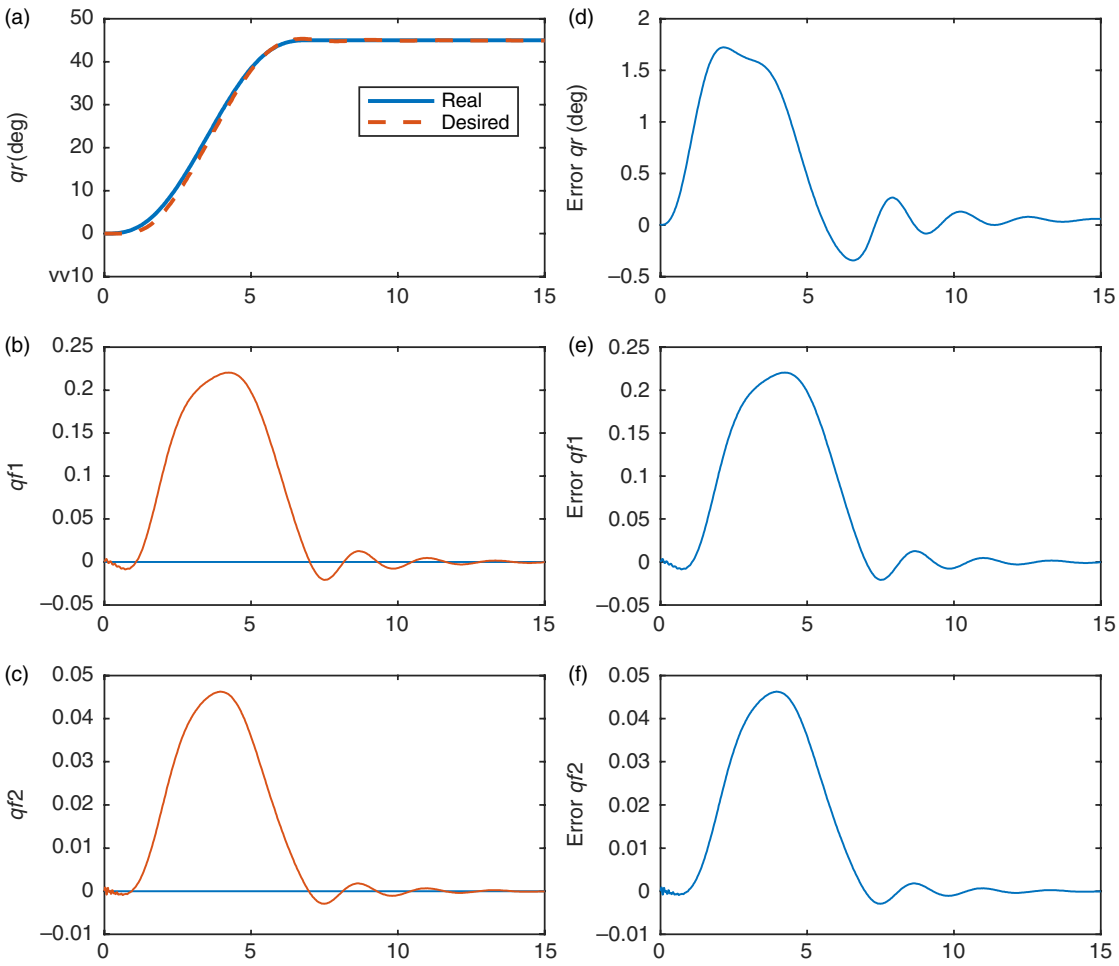

Fig. 8. The computed torque approach.

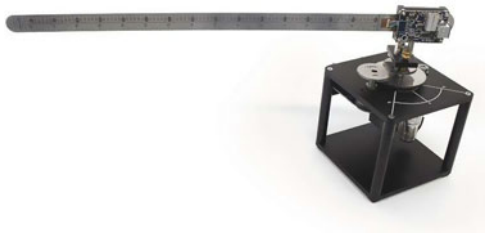

Fig. 9. Single FLM (Quanser FLEXGAGE).

5. Experimental Results

The proposed robust ADRC scheme has been tested experimentally on a single FLM. A photograph of the flexible robot manipulator is shown in Fig. 9. The flexible link robot is a Quanser FLEXGAGE, consisting of the SRV02 Rotary servo base unit and thin stainless-steel beam with strain gauge. The base of the flexible link is mounted on the load gear of the SRV02 system. The servo angle, θ, increases positively when it rotates counter-clockwise (CCW). The servo (and thus the link) turns in the CCW direction when the control voltage is positive, that is, $V_m > 0$. For the flexible link, the gauge is calibrated to output 1 V per inch of tip deflection.

The experimental setup of the flexible-link robot manipulator is shown in Fig. 10. The typical connections used to connect Matlab/Simulink with the flexible link plant to a data-acquisition board and

https://doi.org/10.1017/S026357471900050X Published online by Cambridge University Press

Fig. 10. Experimental setup.

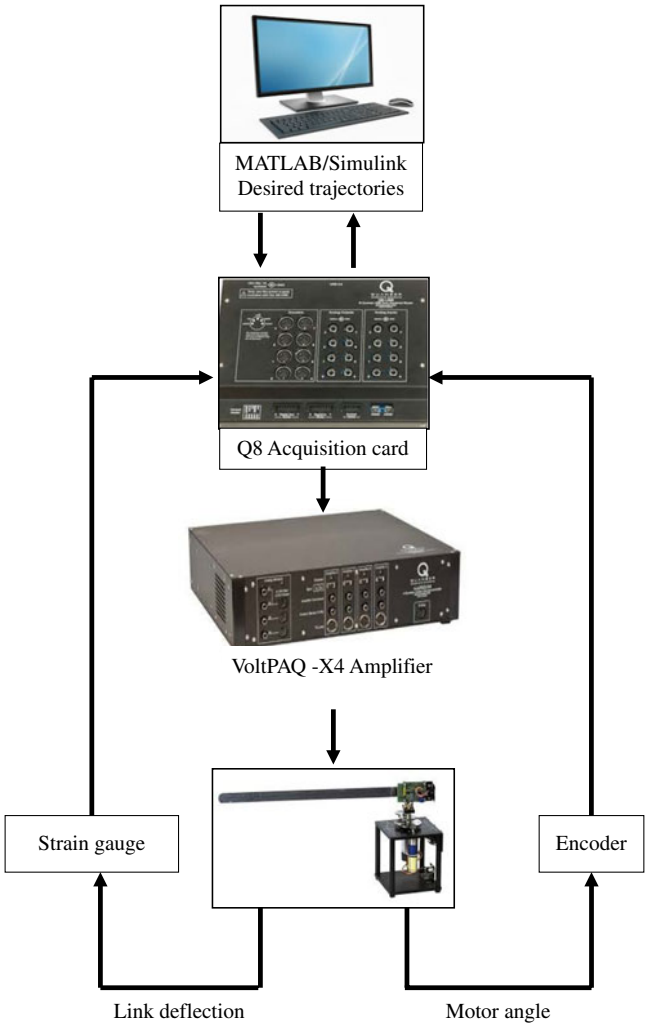

Fig. 11. Flowchart of real time setup.

a power amplifier are given in Fig. 11. It consists of a Q8 terminal board, a DAQ system, sensors such as strain gauges and encoder. The proposed controller is tested in real time using Workshop (RTW) of Mathworks. The experimental results are obtained with $\varepsilon = 0.8$; $b_M = 10$; $b_m = 5 \times 10^{-3}$; $\lambda = 0.2$ and $K_s = 0.04$.

The experimental results using the proposed robust ADRC technique are given in Fig. 12.

The experimental results using the robust ADRC technique, shown in Fig. 12, show a good tracking of the desired trajectories. For the rigid part, Fig. 12(a) shows a good tracking in the joint space and this is confirmed by the tracking error given in Fig. 12(d). For the first and the second mode of the flexible part, Fig. 12(b) and (c) show the tracking trajectories while Fig. 12(e) and (f) show the

https://doi.org/10.1017/S026357471900050X Published online by Cambridge University Press

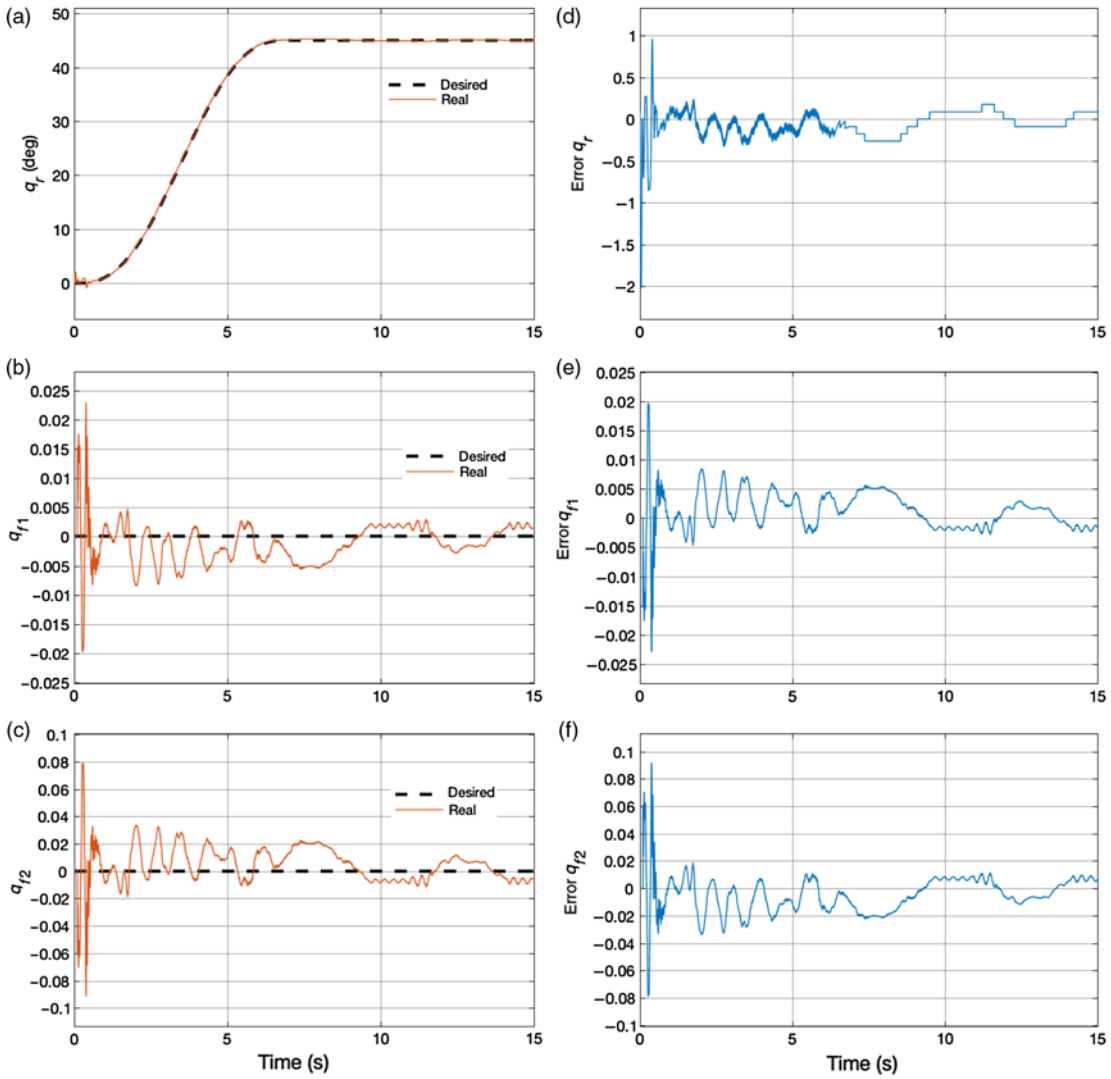

Fig. 12. Experimental results using robust ADRC technique. (a) Tracking trajectory of the rigid part q_r, (b) tracking trajectory of first flexible mode q_{f1}, (c) tracking trajectory of second flexible mode q_{f2}, (d) tracking error of q_r, (e) tracking error of q_{f1} and (f) tracking error of q_{f2}.

associated tracking error. The results show that the tracking errors obtained with the proposed robust ADRC technique are less than 1 deg for the rigid part and close to zero for the flexible part, which is widely tolerable in a lot of practical applications of this kind of systems. Finally, according to these experimental results, we can conclude the effectiveness and good performance of the proposed control strategy.

6. Conclusion

This paper proposed an advanced version of the traditional ADRC strategy applied to FLM. First, the model dynamics of the FLM has been rewritten to take the general form of the traditional ADRC. Then, a robust control technique is designed to overcome two serious limits of the traditional ADRC such as the uncertainty in the knowledge of the control gains; and the presence of the estimation error of the total disturbance which can deteriorate performance of the ADRC. The proposed robust ADRC control law is based on sliding mode technique to solve the problem of the uncertainties and the estimation error. Lyapunov theory has been used to prove the stability of the error dynamics. The proposed robust ADRC was tested experimentally and via numerical simulation on a single FLM. The simulation and experimental results show the effectiveness of the robust ADRC, especially

https://doi.org/10.1017/S026357471900050X Published online by Cambridge University Press

when the system parameters variation and estimation error exist. The effect of the observer bandwidth on the system perform has been simulated and studied to select the best values. A comparison with the tradition ADRC shows the effectiveness of the good performance of the proposed robust ADRC.

References

1. S. Pal, H. E. Stephanou and G. Cook, "Optimal control of a single-link flexible manipulator," *J. Intell. Rob. Syst.* **2**(2–3), 187–199 (1989).
2. R. J. Theodore and A. Ghosal, "Robust control of multilink flexible manipulators," *Mech. Mach. Theory* **38**(4), 367–377 (2003).
3. D. Wang and M. Vidyasagar, "Feedback Linearizability of Multi-link Manipulations with One Flexible Link," *Proceedings of the 28th IEEE Conference on Decision and Control*, Tampa, FL, USA (IEEE, 1989) pp. 2072–2077.
4. M. Moallem, R. V. Patel and K. Khorasani, "An inverse dynamics control strategy for tip position tracking of flexible multi-link manipulators," *J. Rob. Syst.* 14(9), 649–658 (1997).
5. B. Siciliano and W. J. Book, "A singular perturbation approach to control of lightweight flexible manipulators," *Int. J. Rob. Res.* **7**(4), 79–90 (1988).
6. F. L. Lewis and M. Vandegrift, "Flexible Robot Arm Control by a Feedback Linearization/Singular Perturbation Approach," *IEEE International Conference on Robotics and Automation, Proceedings*, Atlanta, GA, USA (IEEE, 1993) pp. 729–736.
7. R. Fareh, M. Saad and M. Saad, "Distributed control strategy for flexible link manipulators," *Robotica* **33**(4), 768–786 (2015).
8. F. Raouf, S. Mohamad, S. Maarouf and B. Maamar, "Distributed adaptive control strategy for flexible link manipulators," *Robotica* **35**(7), 1562–1584 (2017).
9. T. Umeno and Y. Hori, "Robust speed control of DC servomotors using modern two degrees-of-freedom controller design," *IEEE Trans. Ind. Electron.* **38**(5), 363–368 (1991).
10. J. A. Profeta, W. G. Vogt and M. H. Mickle, "Disturbance estimation and compensation in linear systems," *IEEE Trans. Aerosp. Electron. Syst.* **26**(2), 225–231 (1990).
11. S. Kwon and W. K. Chung, "Combined synthesis of state estimator and perturbation observer," *J. Dyn. Syst. Meas. Contr.* **125**(1), 19–26 (2003).
12. Z. Gao, "Active Disturbance Rejection Control: A Paradigm Shift in Feedback Control System Design," *American Control Conference*, Minneapolis, MN, USA (IEEE, 2006) p. 7.
13. Z. Gao, "Scaling and parameterization based controller tuning," *Proceedings of the American Control Conference*, New York, USA (IEEE, 2003) pp. 4989–4996.
14. S. Zheng, B. Han and L. Guo, "Composite hierarchical antidisturbance control for magnetic bearing system subject to multiple external disturbances," *IEEE Trans. Ind. Electron.* **61**(12), 7004–7012 (2014).
15. X. Chang, Y. Li, W. Zhang, N. Wang and W. Xue, "Active disturbance rejection control for a flywheel energy storage system," *IEEE Trans. Ind. Electron.* **62**(2), 991–1001 (2015).
16. J. Yao, Z. Jiao and D. Ma, "Adaptive robust control of DC motors with extended state observer," *IEEE Trans. Ind. Electron.* **61**(7), 3630–3637 (2014).
17. G. Tian and Z. Gao, "Benchmark Tests of Active Disturbance Rejection Control on an Industrial Motion Control Platform," *American Control Conference*, St. Louis, MO, USA (IEEE, 2009) pp. 5552–5557.
18. Q. Zheng and Z. Gao, "An Energy Saving, Factory-Validated Disturbance Decoupling Control Design for Extrusion Processes," *10th World Congress on Intelligent Control and Automation (WCICA)*, Beijing, China (IEEE, 2012) pp 2891–2896.
19. M. Kordasz, R. Madoński, M. Przybyła and P. Sauer, "Active Disturbance Rejection Control for a Flexible-Joint Manipulator," *Robot Motion and Control Conference* (Springer, London, 2012), pp. 247–256.
20. Y. Long, Z. Du, L. Cong, W. Wang, Z. Zhang and W. Dong, "Active disturbance rejection control based human gait tracking for lower extremity rehabilitation exoskeleton," *ISA Trans.* **67**, 389–397 (2017).
21. A. Medjebouri and L. Mehennaoui, "Active disturbance rejection control of a SCARA robot arm," *Int. J. u-and e-Serv., Sci. Technol.* **8**(1), 435–446 (2015).
22. H. Sira-Ramírez, C. López-Uribe and M. Velasco-Villa, "Linear observer-based active disturbance rejection control of the omnidirectional mobile robot," *Asian J. Control* **15**(1), 51–63 (2013).
23. W. J. Book, "Recursive Lagrangian dynamics of flexible manipulator arms," *Int. J. Rob. Res.* **3**(3), 87–101 (1984).
24. M. Benati and A. Morro, "Dynamics of chain of flexible links," *J. Dyn. Syst. Meas. Contr.* **110**(4), 410–415 (1988).
25. M. Saad, O. Akhrif and L. Saydy, "Analytical model of one flexible link system with nonlinear kinematics," *J. Vib. Control* **19**(12), 1795–1806 (2013).
26. B.-Z. Guo and Z.-L. Zhao, "On the convergence of an extended state observer for nonlinear systems with uncertainty," *Syst. Control Lett.* **60**(6), 420–430 (2011).
27. J.-J. E. Slotine and W. Li, *Applied Nonlinear Control*, No. 1 (Prentice Hall, Englewood Cliffs, NJ, 1991).
28. A. D. Luca and B. Siciliano, "Trajectory control of a non-linear one-link flexible arm," *Int. J. Control* **50**(5), 1699–1715 (1989).